International Journal of Fracture **109:** 141–151, 2001.

Structural geometry effect on the size-scaling of strength

SÖREN ÖSTLUND[1] and PETRI KÄRENLAMPI[2]
[1]*Department of Solid Mechanics, Royal Institute of Technology (KTH), SE-10044 Stockholm, Sweden; e-mail: soren@hallf.kth.se*
[2]*Department of Forest Resource Management Box 24, FIN-00014 University of Helsinki, Finland, e-mail: petri.karenlampi@helsinki.fi*

Received 15 March 2000; accepted in revised form 29 September 2000

Abstract. The sensitivity of the empirical exponent of Bazant's size-effect scaling law on structural geometry is clarified through numerical experiments. For large centre- cracked tension panels, made of a linearly softening material, the best-fitting exponent is 0.90, whereas for large edge-cracked panels it is 0.75. For edge-cracked panels, the value of the exponent increases as a function of increasing crack-length-to-width-ratio. The results indicate that with structures of brittleness numbers below unity, reliable predictions of strength require the size-effect scaling law to be fitted for any particular structural geometry.

Key words: Cohesive zone, linear softening, numerical experiments, size effect, structural geometry.

1. Introduction

A possibility of predicting the strength of a structure on the basis of laboratory- measured material characteristics would be desirable. Since strength, *i.e.* the critical nominal stress, depends on the size and geometry of the structure, such effects should somehow be considered.

There is a variety of sources of size effect. The seminal approach by Weibull (1939), discussing statistical size effect, is still the most widely known within the engineering community. Strain gradients, introducing a size effect, may appear due to a variety of structural reasons (Van Vliet and Van Mier, 1999). Size effect may also be due to boundary layer effects, as well as diffusion and hydration phenomena (Bazant and Planas, 1998, p. 9). Fractal geometry explanations have recently been proposed (Carpinteri, 1994a, b; Carpinteri et al., 1994; Carpinteri and Chiaia, 1995). Regardless of the variety of size-effect sources, the deterministic, energetic fracture mechanics size effect often dominates (Bazant and Planas, 1998; Bazant, 2000).

Closed-form solutions are generally available for the geometry effect on the critical nominal stress in two particular cases: the fully plastic case on the one hand, and the Linear Elastic Fracture Mechanics (LEFM) case on the other hand. No analytical solution is available for bridging these asymptotic cases; thus some kind of empirical interpolation is necessary.

Bazant's scaling laws (Bazant, 1984, 1986) combine a description of the energetic size effect and the geometry effect, yielding a prediction on the strength of a structure with a known size, geometry, and a few material parameters. However, the amended form (Bazant, 1986) includes a parameter that has to be determined either empirically or through some more refined theory, cf. Bazant et al. (1999). The appropriate value of the parameter appears to depend on the strain-softening geometry of the material (Bazant and Planas, 1998, p. 266).

Our primary interest is in materials which display approximately linear initial softening, like concrete, mortar and paper (Hillerborg et al., 1976; Swartz et al., 1988; Tryding and Gustafsson, 1996; Tryding, 1996; Kärenlampi and Yu, 1997; Ungsuwarungsri and Knauss, 1988; Östlund and Nilsson, 1993; Planas et al., 1995). Experiments propose that in the case of concrete, the value of the parameter often is in the vicinity of 1 (Bazant et al., 1999). However, no analysis of the eventual geometry-sensitivity of the scaling parameter has so far been presented for such materials. Such an analysis is the objective of this paper.

First, we will briefly review the fracture mechanics size effect and asymptotic solutions for large and small sizes, as well as interpolation formulae. Then, the numerical procedures used in this study are described. Finally, results on the geometry effect on the size scaling of strength, and on the empirical scaling parameter, are reported. No fundamental basis systematising the scanning of eventual geometry effects is known to us, and thus we choose to discuss some well-known geometries: centre-cracked and edge-cracked tension panels.

2. Fracture mechanics size effect

Let us consider a linearly elastic body, of a specified geometry, characterised by a length dimension D, with a through crack of length a. Under invariant external load and boundary displacement, an extension of crack length, da, releases elastic energy by an amount

$$\mathrm{d}U = -\frac{kDb(\sigma^N)^2}{E'}\mathrm{d}a, \tag{1}$$

where k is a geometry-dependent constant, b is the thickness of the structure, σ^N is the nominal stress, and E' is a generalised elastic modulus. On the other hand, at critical circumstances

$$(\mathrm{d}U)_c = -G_f b\ \mathrm{d}a, \tag{2}$$

where G_f is the fracture energy of the material. Thus,

$$G_f = \frac{kD(\sigma_e^N)^2}{E'}, \tag{3}$$

and since G_f is assumed to be a material constant

$$\sigma_c^N \propto D^{-1/2}, \tag{4}$$

where σ_c^N is the critical nominal stress.

The above classical case of the fracture mechanics size effect is, as such, valid as long as Linear Elastic Fracture Mechanics (LEFM) is valid. LEFM is valid as long as all characteristic dimensions of the structure are large in comparison to the size of the fracture process zone, and possibly a plastic yielding zone surrounding the crack-tip. The size of the process zone in turn depends on material properties. Following Hillerborg et al. (1976), we define a *characteristic material length* as

$$l_{ch} = \frac{G_f E'}{\sigma_c^2}, \tag{5}$$

where σ_c is the tensile strength of the material, corresponding to the stress at the initiation of strain softening.

Now, Equation (4) is valid as long as $D/l_{ch} = \infty$. Under the same circumstances, $\sqrt{G_f E'} = K_c = \sigma_c^N \sqrt{a}\beta$, where β is a geometry-dependent function. In case $D/l_{ch} < \infty$, we assume the deviation from LEFM in the form of a power series

$$\frac{G_f E'}{\left(\sigma_c^N \sqrt{a}\beta\right)^2} = 1 + c_1 \frac{l_{ch}}{D} + c_2 \left(\frac{l_{ch}}{D}\right)^2 + c_3 \left(\frac{l_{ch}}{D}\right)^3 + \cdots . \tag{6}$$

In the case $l_{ch}/D \to 0$, the power series may be truncated to first order, and we get

$$\sigma_c^N = \frac{\eta_\infty \sigma_c}{\sqrt{1 + \theta_\infty \dfrac{D}{l_{ch}}}} \quad \text{for } \frac{l_{ch}}{D} \to 0, \tag{7}$$

where η_∞ and θ_∞ are dimensionless variables, depending on material properties and on the geometry of the structure, but being independent on the size of the structure. Equation (7) gives the asymptotic solution for the critical nominal stress in the vicinity of a LEFM solution. Analytical solutions for the variables η_∞ and θ_∞ are available in the literature, see for example (Planas and Elices, 1991, 1992; Elices and Planas, 1992; Planas et al., 1997; Bazant and Planas, 1998).

3. Small-size asymptotic and interpolation formulae

In the limit of small structures with only one characteristic length, we can possibly write (Bazant and Planas, 1998; Bazant, 1984, 1986),

$$\frac{\sigma_c^N}{\sigma_c} = \eta_0 + \eta_1 \frac{D}{l_{ch}} + \eta_2 \left(\frac{D}{l_{ch}}\right)^2 + \eta_3 \left(\frac{D}{l_{ch}}\right)^3 + \cdots . \tag{8}$$

Since $D/l_{ch} \to 0$, the power series may be truncated, and we get

$$\sigma_c^N = \frac{\eta_0 \sigma_c}{\sqrt{1 + \theta_0 \dfrac{D}{l_{ch}}}} \quad \text{for} \quad \frac{D}{l_{ch}} \to 0, \tag{9}$$

where η_0 and θ_0 are dimensionless variables, depending on material properties and structural geometry, but not on the size of the structure.

In many cases, the analytical solution for η_0 is straightforward, since in the absence of elastic stress concentrations, $\eta_0 \sigma_c$ equals the limit load achievable through a fully plastic analysis. However, unlike for θ_∞, with the exception of some special cases, no analytical solutions are available for θ_0. In general, the latter variable can be determined only numerically. Further, in the absence of analytical support, there is no guarantee that the integer power series Equation (9) describes the asymptotic deviation from the fully plastic solution for the critical nominal stress. Actually, it has been shown numerically by Planas et al. (1997) that in the case of an initially linearly softening cohesive law, the appropriate asymptotic formula for three-point bending specimens is

$$\sigma_c^N = \frac{\eta_0 \sigma_c}{\sqrt{1 + \sqrt{\mu_0 \dfrac{D}{l_{ch}}}}} \quad \text{for} \quad \frac{D}{l_{ch}} \to 0, \tag{10}$$

where μ_0 depends on material properties and structural geometry.

In 1984, Bazant (1984) implicitly assumed that $\eta_\infty = \eta_0$ and $\theta_\infty = \theta_0$, which, through asymptotic matching, resulted in the size-effect scaling law

$$\sigma_c^N = \frac{\sigma_c^{pl}}{\sqrt{1+B}}, \tag{11}$$

where σ_c^{pl} is fully plastic solution for the critical nominal stress, and B is the *brittleness number*. Asymptotic matching at the LEFM limit yields

$$B = \frac{\left(\sigma_c^{pl}\right)^2 D}{G_f E'} g, \tag{12}$$

where g is a dimensionless geometry function. Using the notation of Equation (6),

$$g = \frac{a}{D}\beta^2.$$

In order to achieve a better fit to experimental results, Bazant (1986) later modified the scaling law of Equation (11) into the more flexible form

$$\sigma_c^N = \frac{\sigma_c^{pl}}{(1+B^r)^{1/2r}} \tag{13}$$

which, of course, provides the same asymptotes at the plastic and the LEFM limits. Anyway, the assumptions, $\eta_\infty = \eta_0$ and $\theta_\infty = \theta_0$, are not well justified; very different mechanisms prevail in the vicinity of the plastic limit and the LEFM limit. Thus, the asymptotic matching is a questionable procedure in this case.

In addition to Equations (11) and (13), more complicated interpolation formulae have been presented in the literature (Planas et al., 1997). However, such formulae have to be calibrated for any structural geometry, as well as for any strain-softening behaviour. The relative simplicity of Equation (13) makes it very attractive, at least if the scaling exponent r would not be strongly dependent on structural geometry. In the following sections, we intend to study the structural geometry effect on r in the case of linearly softening materials.

4. Numerical procedures

Numerical analyses were accomplished for centre-cracked and edge-cracked tension panels under plane stress. The mathematical model is described in detail in (Östlund and Nilsson, 1993; Östlund, 1995), the crack-tip singularity being cancelled by the action of the cohesive stresses. The notations used for the mathematical formulation are shown in Figure 1.

The equation governing the crack widening was derived by considering the closing action of the cohesive forces acting on the surface of the crack. Normalised crack widening, $\hat{v} = v/v_c$, is determined from the solution of the integral equation

$$\hat{v}(\overline{x}) = \frac{\sqrt{\overline{w}}}{\sqrt{\pi \overline{a}_0}} \frac{f_v\left(\frac{\overline{x}}{\overline{w}}, \frac{\overline{a}}{\overline{w}}\right)}{f_k\left(\frac{\overline{a}_0}{\overline{w}}, \frac{\overline{a}}{\overline{w}}\right)} \int_{\overline{a}_0}^{\overline{a}} \hat{p}(\hat{v}) g_k\left(\frac{\overline{\xi}}{\overline{w}}, \frac{\overline{a}}{\overline{w}}\right) \mathrm{d}\overline{\xi} - \int_{\overline{a}_0}^{\overline{a}} \hat{p}(\hat{v}) g_v\left(\frac{\overline{\xi}}{\overline{w}}, \frac{\overline{x}}{\overline{w}}, \frac{\overline{a}}{\overline{w}}\right) \mathrm{d}\overline{\xi}, \tag{14}$$

where an uppercase bar denotes normalisation with respect to l_{ch}. The normalised cohesive stress is given by the linear softening law

$$\hat{p} = \frac{p}{\sigma_c} = 1 - \hat{v}. \tag{15}$$

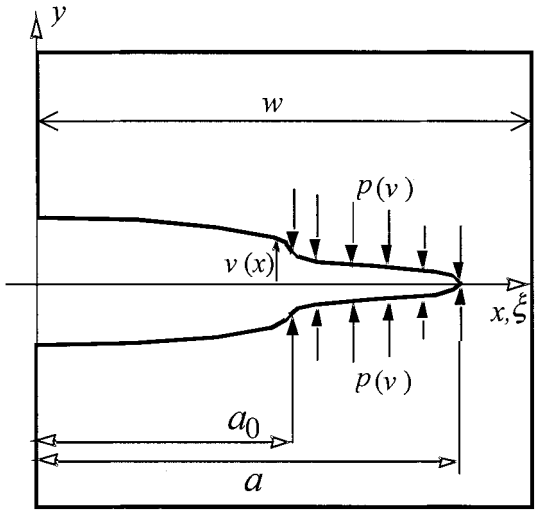

Figure 1. Cohesive zone modelling of bridging at a loaded crack tip.

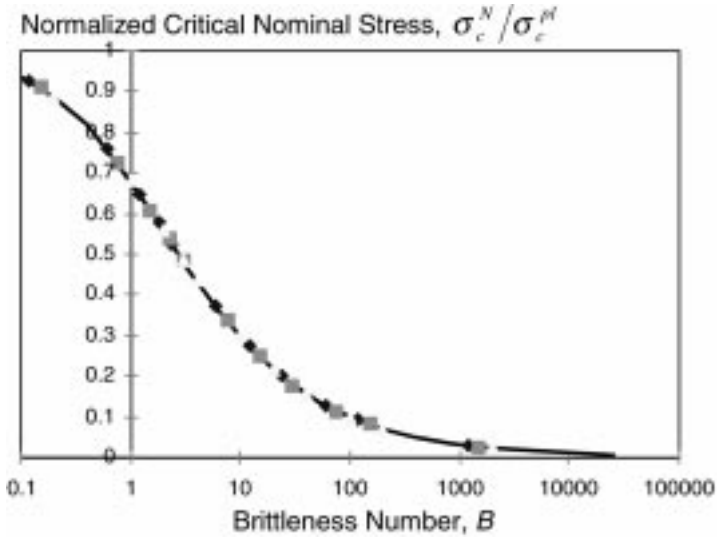

Figure 2. Results of numerical experiments for the critical nominal stress within a large centre-cracked tension panel as a function of brittleness number, as well as a fit of Equation (13) into the results. The analysis is carried out with a linearly softening cohesive law and the curve fit yields the exponent $r = 0.9$.

The functions f_v and f_k are defined by the crack widening $V(x)$ and stress intensity factor K, respectively, which would result from a crack of length a, without any bridging forces:

$$V(x) = \frac{\sigma^N}{E'} w f_v\left(\frac{x}{w}, \frac{a}{w}\right), \tag{16}$$

$$K = \sigma^N \sqrt{\pi a_0} f_k\left(\frac{a_0}{w}, \frac{a}{w}\right). \tag{17}$$

The functions f_v and f_k are given in the Appendix. The functions g_v and g_k are Green's functions, which are also given in the Appendix.

By increasing the external tensile load and thus the applied stress intensity factor, equilibrium solutions to Equation (14) for the length of the damage zone, as well as crack widening

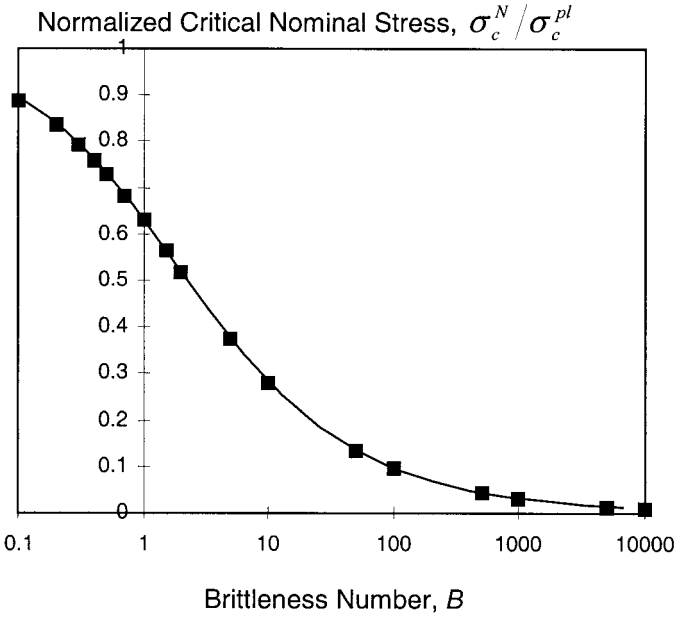

Figure 3. Results of numerical experiments for the critical nominal stress within a large double-edge-cracked tension panel as a function of brittleness number, as well as a fit of Equation (13) into the results. The analysis is carried out with a linearly softening cohesive law and the curve fit yields the exponent $r = 0.75$.

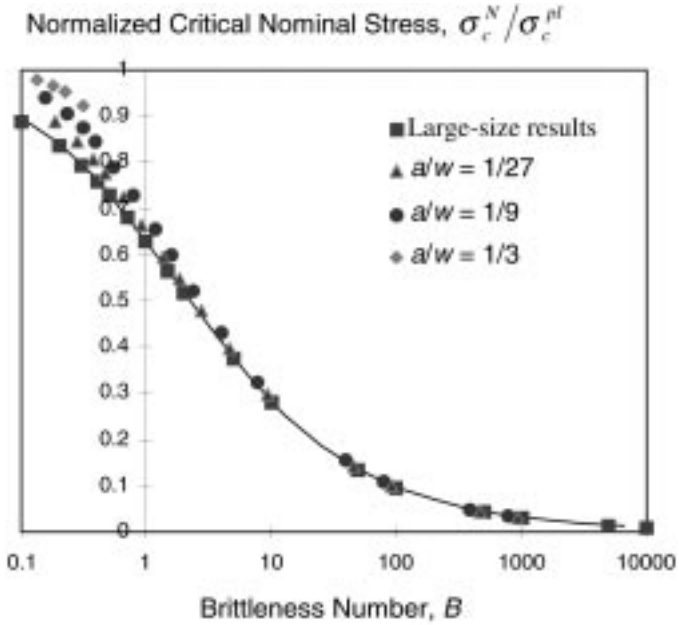

Figure 4. Results of numerical experiments for double-edge-notched tension panels with three different geometries, in addition to the large-size results already shown in Figure 3. The analysis is carried out with a linearly softening cohesive law.

and the resulting cohesive stress within the damage zone, were searched. This was repeated, for increased external load, unless instability occurred. A detailed description of the numerical procedure used for solving the integral equation is available in a previous paper (Östlund, 1995).

5. Results

Numerical results for the normalised critical nominal stress σ_c^N/σ_c^{pl} within a large centre-cracked panel, as a function of the brittleness number, are shown in Figure 2. Figure 2 also shows a fit into Equation (13); an exponent $r = 0.9$ provides an excellent fit to the numerical results.

Numerical results for the normalised critical nominal stress σ_c^N/σ_c^{pl} within a large double-edge-cracked tension panel, as a function of the brittleness number, are shown in Figure 3. Figure 3 also shows a fit into Equation (13); an exponent $r = 0.75$ provides an excellent fit with the numerical results. We find that the normalised critical stress is lower for the double edge-cracked panel (Figure 3) than for the centre-cracked panel (Figure 2).

It appears from the above that there possibly is a significant structural geometry effect on the empirical scaling exponent. In order to verify this, computer experiments were conducted for three additional geometries of double edge-cracked tension panels, for crack-length-to-half-width ratios $a/w = \frac{1}{3}$, $a/w = \frac{1}{9}$, and $a/w = \frac{1}{27}$. The results, together with the infinite-panel result, are shown in Figure 4. We find that there definitely is a geometry effect: the critical stress is greater for large a/w-ratios. The necessary scaling exponent increases as well, being in the order of 1.3-1.4 for $a/w = \frac{1}{3}$.

6. Discussion

Even with invariant material properties, the size-scaling of strength is sensitive to structural geometry. With structures of brittleness numbers below unity, reliable predictions of strength require the size-effect scaling law to be fitted for any particular structural geometry. This somewhat reduces the applicability of Bazant's scaling law (Bazant, 1986) for the prediction of the strength of structures.

We find from Figure 4 that the structural geometry effect on the size-scaling of strength vanishes at large brittleness numbers. This is a natural consequence of the brittleness number being matched to the LEFM limit. The large-brittleness asymptote of the scaling thus is correct and exactly known. The same matching not really being valid at low brittlenesses, the scaling loses its generality when the brittleness number decreases to the vicinity of unity.

In an ideal situation, the strength of a structure could be determined on the basis of laboratory-measured material properties using a simple scaling law, without entering numerical exercises. Unfortunately, this does not appear to be possible. When the structural geometry is variable, size-scaling always appears to require parameters which have to be determined numerically.

Acknowledgements

Professor Fred Nilsson is gratefully acknowledged for reading through the manuscript and giving suggestions for improvements.

References

Bazant, Z.P. (1984). Size effect in blunt fracture: concrete, rock, metal. *Journal of Engineering Mechanics* **110**, 518–535.

Bazant, Z.P. (1986). Fracture mechanics and strain-softening of concrete. *Proceedings, U.S.-Japan Seminar on Finite Element Analysis of Reinforced Concrete Structures* (Tokyo, May 1985). American Society of Civil Engineers, New York, 121–150.

Bazant, Z.P. (2000). Size effect. *International Journal of Solids and Structures* **37**, 69–80.

Bazant, Z.P. and Planas, J. (1998). *Fracture and size effect in concrete and other quasibrittle materials*. CRC Press.

Bazant, Z.P., Kim, J.-J. H., Daniel, I.M., Becq-Giraudon, E. and Li, G. (1999). Size effect on compression strength of fiber composites failing by kink band propagation. *International Journal of Fracture* **95**, 89–101.

Carpinteri, A. (1994a). Scaling laws and renormalization groups for strength and toughness of disordered materials. *International Journal of Solids and Structures* **31**, 291–302.

Carpinteri, A. (1994b) Fractal nature of material microstructure and size effects on apparent mechanical properties. *Mechanics of Materials* **18**, 89–101.

Carpinteri, A., Chiaia, B. and Ferro, G. (1994). Multifractal nature of material microstructure and size effect on nominal tensile strength. *Fracture of Brittle Disordered Materials: Concrete, Rock and Ceramics* (Edited by G. Baker and B. L. Karihaloo). E&FN Spon, London, 21–34.

Carpinteri, A. and Chiaia, B. (1995). Multifractal scaling law for the fracture energy variation of concrete structures. *Fracture mechanics of concrete structures* (Edited by F.H. Wittmann). Aedificatio Publishers, Freiburg, Germany, 581–569.

Elices, M. and Planas, J. (1992). Size effect in concrete structures: an R-curve approach. *Applications of Fracture Mechanics to Reinforced Concrete* (Edited by A. Carpinteri). Elsevier Applied Science, London, 169–200.

Hillerborg, A., Modéer, M. and Petersson, P.-E. (1976). Analysis of crack formation in concrete by means of fracture mechanics and finite elements. *Cement and Concrete Research* **6**, 773–782.

Kärenlampi, P. and Yu, Y. (1997). Fiber properties and paper fracture - fiber length and fiber strength. *11th Fundamental Research Symposium*, Cambridge, England, September 23–26, 1997, 521–545.

Östlund, S. and Nilsson, F. (1993). Cohesive modelling of process regions for cracks in linear elastic structures - fundamental aspects. *Fatigue and Fracture of Engineering Materials and Structures* **16**, 215–235.

Östlund, S. (1995). Fracture modelling of brittle-matrix composites with spatially dependent crack bridging. *Fatigue and Fracture of Engineering Materials and Structures* **18**, 1213–1230.

Planas, J. and Elices, M. (1991). Nonlinear fracture of cohesive materials. *International Journal of Fracture* **51**, 139–157.

Planas, J. and Elices, M. (1992). Asymptotic analysis of a cohesive crack: 1. Theoretical background. *International Journal of Fracture* **55**, 153–177.

Planas, J., Guinea, G.V. and Elices, M. (1995). Rupture modulus and fracture properties of concrete. *Fracture mechanics of concrete structures* (Edited by F.H. Wittmann). Aefiticatio Publishers, Freiburg, Germany, 95–110.

Planas, J., Guinea, G.V. and Elices, M. (1997). Generalized size effects equation for quasibrittle materials. *Fatigue and Fracture of Engineering Materials and Structures* **20**, 671–687.

Swartz, S.E., Lu, L.W. and Tang, L.D. (1988). Mixed-mode fracture toughness testing of concrete beams in three-point bending. *Materials and Structures* **21**, 33–40.

Tada, H. (1985). *The Stress Analysis of Cracks Handbook*. Paris Productions, St. Louis, Missouri, U.S.A.

Tryding, J. and Gustafsson, P.-J. (1996). Localized damage and fracture in paper. *1996 International Paper Physics Seminar*, Stockholm, Sweden, 144–150.

Tryding, J. (1996). *In-plane fracture of paper*. Lund University, Division of Structural Mechanics, Report TVSM-1008.

Ungsuwarungsri, T. and Knauss, W.G. (1988). A nonlinear analysis of an equilibrium craze: Part II - Simulations on craze and crack growth. *Journal of Applied Mechanics* **55**, 42–58.

Van Vliet, M.R.A. and Van Mier, J.G.M. (1999). Effect of strain gradients on the size effect on concrete in uniaxial tension. *International Journal of Fracture* **95**, 195–219.

Weibull, W. (1939). A statistical theory on the strength of materials. *Ingenjörsvetenskapsakademins handlingar*, **151**, 5–45.

Wu, X.-R. and Carlsson, J. (1991). *Weight Functions and Stress Intensity Factor Solutions*. Pergamon Press, Oxford, U.K.

Appendix

Geometry-specific functions used in the formulation of the governing equations are given in this appendix. The expressions for a central crack in an infinite plate under remote uniform tension are exact and can be found in Tada (1985). The solutions for a double-edge-cracked finite plate under remote uniform tension are approximate high accuracy solutions obtained using a weight function technique (Wu and Carlsson, 1991). It should be noted that the analysis for double-edge-cracked-infinite width plate under uniform remote tension was carried out by considering a finite width plate of sufficient width to yield results independent of the width of the plate.

CENTRE-CRACKED INFINITE PLATE UNDER REMOTE UNIFORM TENSION

$$f_k\left(\frac{a_0}{w}, \frac{a}{w}\right) = \sqrt{\frac{a/w}{a_0/w}}, \tag{A1}$$

$$f_v\left(\frac{x}{w}, \frac{a}{w}\right) = 2\sqrt{\left(\frac{a}{w}\right)^2 - \left(\frac{x}{w}\right)^2}, \tag{A2}$$

$$g_k\left(\frac{\xi}{w}, \frac{a}{w}\right) = \frac{2}{\sqrt{\pi}} \frac{\sqrt{\frac{a}{w}}}{\sqrt{\left(\frac{a}{w}\right)^2 - \left(\frac{\xi}{w}\right)^2}}, \tag{A3}$$

$$g_v\left(\frac{\xi}{w}, \frac{x}{w}, \frac{a}{w}\right) = \frac{4}{\pi} \log\left(\frac{\sqrt{\left(\frac{a}{w}\right)^2 - \left(\frac{x}{w}\right)^2} + \sqrt{\left(\frac{a}{w}\right)^2 - \left(\frac{\xi}{w}\right)^2}}{\sqrt{\left|\frac{\xi^2}{w} - \frac{x^2}{w}\right|}}\right). \tag{A4}$$

DOUBLE-EDGE-CRACKED FINITE WIDTH PLATE UNDER UNIFORM REMOTE TENSION

$$f_k\left(\frac{a_0}{w}, \frac{a}{w}\right) = f_r\left(\frac{a}{w}\right) \cdot \sqrt{\frac{a/w}{a_0/w}}, \tag{A5}$$

where

$$f_r\left(\frac{a}{w}\right) = \frac{\sum_{i=0}^{6} \alpha_i \left(\frac{a}{w}\right)^i}{\sqrt{1 - \frac{a}{w}}} \tag{A6}$$

and $\alpha_0 = 1.1215, \alpha_1 = -0.5699, \alpha_2 = -0.7056, \alpha_3 = 2.4748, \alpha_4 = -3.1194, \alpha_5 = 1.8945, \alpha_6 = -0.4594$.

$$f_v\left(\frac{x}{w},\frac{a}{w}\right)=\frac{a}{w}\sqrt{\frac{1-\frac{x}{a}}{2}}\sum_{j=1}^{4}F_j\left(\frac{a}{w}\right)\cdot\left(1-\frac{x}{a}\right)^{j-1}, \tag{A7}$$

where

$$F_1\left(\frac{a}{w}\right)=4f_r\left(\frac{a}{w}\right), \tag{A8}$$

$$F_2\left(\frac{a}{w}\right)=\frac{1}{12\sqrt{2}}\left[315\pi\phi\left(\frac{a}{w}\right)-105V_r\left(\frac{a}{w}\right)-208\sqrt{2}f_r\left(\frac{a}{w}\right)\right], \tag{A9}$$

$$F_3\left(\frac{a}{w}\right)=\frac{1}{30\sqrt{2}}\left[-1260\pi\phi\left(\frac{a}{w}\right)+525V_r\left(\frac{a}{w}\right)+616\sqrt{2}f_r\left(\frac{a}{w}\right)\right], \tag{A10}$$

$$F_4\left(\frac{a}{w}\right)=\sqrt{2}V_r\left(\frac{a}{w}\right)-\left[F_1\left(\frac{a}{w}\right)+F_2\left(\frac{a}{w}\right)+F_3\left(\frac{a}{w}\right)\right]. \tag{A11}$$

Furthermore

$$\phi\left(\frac{a}{w}\right)=\frac{1}{\left(\frac{a}{w}\right)^2}\int_0^{a/w}s\left[f_r(s)\right]^2\mathrm{d}s \tag{A12}$$

and

$$V_r\left(\frac{a}{w}\right)=\left[\sum_{n=0}^{7}\gamma_n\left(\frac{a}{w}\right)^n\right]\Bigg/\left(1-\frac{a}{w}\right)^2 \tag{A13}$$

where $\gamma_0=2.9086$, $\gamma_1=-1.2338$, $\gamma_2=-3.6484$, $\gamma_3=6.4738$, $\gamma_4=12.2265$, $\gamma_5=-54.9146$, $\gamma_6=65.9937$, $\gamma_7=-27.070$.

$$g_k\left(\frac{\xi}{w},\frac{a}{w}\right)=\frac{1}{\sqrt{\pi\frac{a}{w}}}\sqrt{\frac{1-\frac{x}{a}}{2}}\sum_{i=1}^{5}\beta_i\left(\frac{a}{w}\right)\cdot\left(1-\frac{x}{a}\right)^{i-2}, \tag{A14}$$

where

$$\beta_1\left(\frac{a}{w}\right)=2.0, \tag{A15}$$

$$\beta_2\left(\frac{a}{w}\right)=\left[4\frac{a}{w}f_r'\left(\frac{a}{w}\right)+2f_r\left(\frac{a}{w}\right)+\frac{3}{2}F_2\left(\frac{a}{w}\right)\right]/f_r\left(\frac{a}{w}\right), \tag{A16}$$

$$\beta_3\left(\frac{a}{w}\right)=\left\{\frac{a}{w}F_2'\left(\frac{a}{w}\right)+\frac{1}{2}\left[5F_3\left(\frac{a}{w}\right)-F_2\left(\frac{a}{w}\right)\right]\right\}/f_r\left(\frac{a}{w}\right), \tag{A17}$$

$$\beta_4\left(\frac{a}{w}\right)=\left\{\frac{a}{w}F_3'\left(\frac{a}{w}\right)+\frac{1}{2}\left[7F_4\left(\frac{a}{w}\right)-3F_3\left(\frac{a}{w}\right)\right]\right\}/f_r\left(\frac{a}{w}\right), \tag{A18}$$

$$\beta_5\left(\frac{a}{w}\right)=\left\{\frac{a}{w}F_4'\left(\frac{a}{w}\right)-\frac{5}{2}F_4\left(\frac{a}{w}\right)\right\}/f_r\left(\frac{a}{w}\right), \tag{A19}$$

$$g_v\left(\frac{\xi}{w}, \frac{x}{w}, \frac{a}{w}\right) = \frac{1}{2\pi} \int_{a_0/w}^{a/w} \frac{s \sum_{i=1}^{5} \beta_i(s) \left[1 - \frac{\xi/w}{s}\right]^{i-1} \cdot \sum_{i=1}^{5} \beta_i(s) \left[1 - \frac{x/w}{s}\right]^{i-1}}{\sqrt{\left(s - \frac{\xi}{w}\right)\left(s - \frac{x}{w}\right)}} \mathrm{d}s. \qquad \text{(A20)}$$